Development of x-ray emission computed tomography for ICF research

M. Nakai, S. Shinohara, M. Katayama, Y.-W. Chen, S. Kobayashi, N. Miyanaga, K. A. Tanaka, K. Nishihara, M. Yamanaka, T. Yamanaka, and S. Nakai
Institute of Laser Engineering, Osaka University, Suita Osaka 565, Japan

(Presented on 7 May 1990)

A computed tomographic (CT) technique has been developed to diagnose laser-irradiated spherical targets using x-ray emissions. The three-dimensional (3-D) x-ray distribution was reconstructed by using an algebraic reconstruction technique (ART) from x-ray pinhole camera images obtained along different sight directions. 3-D distributions of electron temperature and density were measured by use of an absorption filter technique. Time-resolved 3-D x-ray emission images from an imploding hollow shell target were reconstructed with less than 100 ps temporal resolution by using x-ray multiframing cameras.

I. INTRODUCTION

It has been recognized that the compression of the liquid fuel (deuterium and/or tritium) up to 500–1000 times the liquid density is necessary to ignite thermonuclear burn in an inertial confinement pellet. Implosion uniformity is a key issue for achievement of such a high compression. Shapes of the imploding pellet and compressed core plasma have been observed by x-ray and particle imaging diagnostics.[1,2] But a single image could only give two-dimensional information integrated along a particular direction. In order to evaluate the three-dimensional nonuniformity, a tomographic technique is desired. We have developed a computed tomographic (CT) technique to reconstruct the three-dimensional x-ray emission distribution from several x-ray pictures taken by x-ray pinhole cameras from different directions.

The implosion process is completed in a very short time, typically 1 ns. Therefore it is impossible to use a moving detector, as is used in the medical research, to spatially scan the object. In implosion experiments many kinds of detectors are attached to the vacuum chamber, in the center of which the pellet target is irradiated by energy drivers. All the required data must be acquired simultaneously in a single shot using a limited number of detectors. Thus, measurement of the 3-D x-ray emission distribution is a reconstruction problem from incomplete projection data with some *a priori* constraints. We have adopted an algebraic reconstruction technique as an algorithm because it can manage a large matrix of data and incorporate *a priori* knowledge into the reconstruction procedure.[3-6] Spectral information can be used to determine plasma parameters. Here we use information obtained from a set of filtered images to obtain the 3-D distributions of electron temperature and relative density.

In order to perform the computed tomography, it is necessary to develop accurate detectors with rapid data analysis capability. When nonlinear functions are included in the projection measurements, various distorting artifacts having distinctive shapes are produced through reconstruction processes.[7,8] Therefore we designed two types of x-ray image detectors with CCD (charge coupled device) cameras.[9,10] The first is just a phosphor, which provides time-integrated signals but has constant spectral sensitivity suitable for the absorption filter method. The other is an x-ray framing camera, which provides temporal resolution better than 100 ps. Using the CCD cameras as image detectors, the direct acquisition system can be constructed.

In this paper, after the description of the x-ray CT system on the Gekko XII facility at ILE Osaka, we present examples reconstructing the 3-D temperature distribution.

II. SYSTEM CONSTRUCTION

The x-ray CT system for implosion experiments at ILE consists of pinhole adjusters, x-ray imaging detectors, CCD camera sets, and frame memories (Fig. 1). Each two-dimensional image is accumulated from the CCD in a frame memory, then transferred to the main computer (NEC-ACOS). The set of two-dimensional images is then reconstructed to obtain a 3-D image. Each x-ray imaging detector is coupled to a thermoelectrically cooled CCD camera through relay lens optics ($F/2$). The CCDs and frame memories are commercially available (Hamamatsu, C3140 and C3610). The CCD has a 510×492 pixel format in an area of 8.6×6.6 mm^2. They are used at a frame rate of 1 Hz, signal charge is accumulated on each pixel for 1 s, then digitized by a 12 bit A/D converter. The rms noise levels are below 50 electrons/pixel at -30 °C and specified dynamic range is more than 2000.

Two types of x-ray image converters are used. The first is an optical flat overcoated with P20 phosphor [(Zn, Cd)S:Ag] of 10 μm in thickness. Grain size of the phosphor was about 2 μm. Magnification of the relay optics was designed to be 1/2 and the effective area on the phosphor was 17×13 mm^2. The second type of detector is a multiframe framing camera.[11] This is a gated microchannel plate (MCP) image converter, which consists of a pair

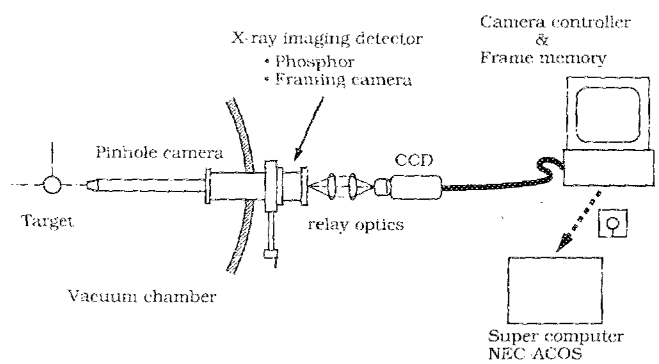

FIG. 1. Schematic diagram of the x-ray CT system on Gekko XII.

of MCPs and a phosphor screen. The first MCP is used as a gated photocathode with its electrode in a strip line configuration gated by an electric pulse; the second MCP is an electron multiplier as usual. Images are formed along the strip line by a pinhole array at the time when the electric pulse passes through each point. Thus we can obtain six sequential temporally resolved images with a time interval of 100 ps. According to the experimental result using the 4th harmonic of a glass laser with a pulse duration of about 10 ps, the temporal resolution was about 80 ps and the dynamic range was more than 10^2 with linearity within an error of $\pm 20\%$. The spatial resolution was evaluated to be 10 lp/mm (at MTF $= 20\%$) by measuring the modulation transfer function.

Reconstruction of 3-D x-ray emission distribution uses an inversion technique to estimate a 3D distribution $I(x,y,z)$ from its several 2D projections. Since the visual angle of each pinhole camera is very small, we can regard our system as in parallel geometry. Assuming that the self-absorption of x rays within the plasma in question is negligible, obtained images are regarded as parallel projections along the viewing directions. In order to determine the three-dimensional distribution $I(x,y,z)$ from such two-dimensional projections obtained at different viewing directions, an iterative method known as the multiplicative algebraic reconstruction technique was used.[2]

The major advantage of ART is that *a priori* knowledge can be incorporated into the reconstruction procedure.[4] As the constraints, we incorporated a positivity and boundary condition; the kth reconstruction I^k should be zero outside the initial target. Namely, in each iteration negative I^ks and I^ks outside the initial target radius were set to be zero.

In order to evaluate the accuracy of the reconstruction, computer simulations were performed using the phantom shown in Fig. 2 (a). The phantom contains two spheres of relative intensities 1, 3 and relative radii 24, 9, respectively. The central intense sphere [shaded area in Fig. 2(a)] has been truncated and shifted by three pixels from the center along for each x, y, and z axis respectively on purpose. The averaged intensity error $\delta I/I$ (rms) and the averaged deviation of the size of center core [shaded area in Fig. 2(a)] $\delta R/R$ between the original object and reconstructed image were calculated [Fig. 2(b)]. The dashed lines and solid lines show the accuracy of reconstruction with and without addition of Poisson noise to each projection, where the signal-to-noise ratio was assumed to be 10. As seen in the figure, the accuracy of reconstruction is improved by increasing the number of detectors, the deviations $\delta I/I$ and $\delta R/R$ are estimated to be $\sim 30\%$ and $\sim 16\%$ with three detectors. Another measure of the reconstruction accuracy is shown in Fig. 3. Spread of a point source in FWHM is shown as the spatial resolution in the figure. The solid square is an experimental value obtained from the spread of the surface emission of a plastic shell target (800 μm in diameter) irradiated by short-pulse (100 ps FWHM) laser beams. The spatial resolution of about 40 μm was provided using three pinhole cameras.

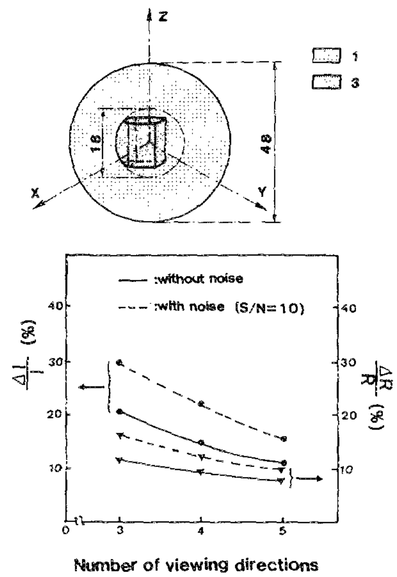

FIG. 2. Reconstruction accuracy was evaluated by computer simulation using a phantom (a). The intensity error ($\delta I/I$) and the core size deviation ($\delta R/R$) between the reconstructed image and original object are improved with increasing the number of viewing directions.

If the absorption opacity of the object plasma can be neglected, the emission coefficient at each point is derived by the method described above. Knowing the spectral emission coefficient we can calculate the temperature and density of the plasma. When the x-ray photon energy $h\nu$ in the observed region is higher than the ionization energy of the plasma, the dominant radiation process is bremsstrahlung. In such a situation one can obtain the electron temperature of the plasma by the absorption filter technique. Assuming a Maxwellian electron-energy distribution, the spectral emission coefficient due to bremsstrahlung is described as a function of electron density n_e and temperature T_e. The three-dimensional distribution $I(x,y,z)$ reconstructed from the projections taken by the detector with the spectral sensitivity $S(\nu)$ through an absorption filter of the thickness l is

$$I(x,y,z) \propto \frac{Z}{kT_e(x,y,z)}\, n_e(x,y,z)^2 \exp\left(-\frac{h\nu}{kT_e(x,y,z)}\right) \times \exp[-\mu(h\nu)l]S(\nu)d\nu, \quad (1)$$

where $\mu(h\nu)$ is a mass absorption coefficient of the filter material. Therefore the ratios $R(x,y,z)$s among I (x,y,z)s

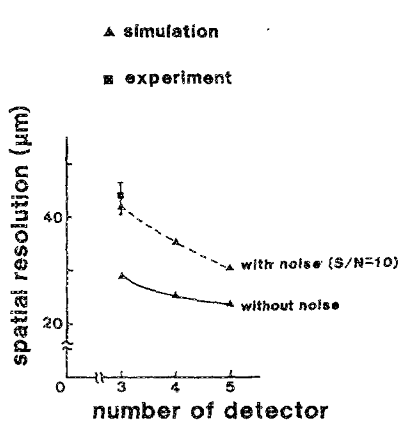

FIG. 3. Full width of the half maximum of the reconstructed image of a point emission was calculated varying the number of the viewing directions, as the measure of the spatial resolution.

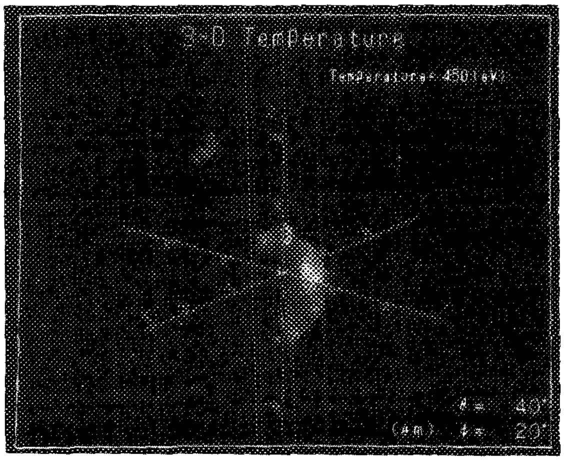

FIG. 4. 3-D display of the 450 eV isotemperature surface in the imploded core of a cryogenic foam shell target.

obtained from the projections using absorption filters of different thicknesses are not dependent on n_e but a function of T_e. Thus one can obtain the temperature $T_e(x,y,z)$ from the ratio $R(x,y,z)$. The relative density distribution can then be obtained from Eq. (1). It is very difficult to calculate the density distribution directly because it is difficult to absolutely calibrate the detectors. The absolute value could be deduced by knowing the residual mass or density-radius product from other measurements.

III. APPLICATIONS

In order to measure the time-integrated three-dimensional temperature distribution in the imploded core plasma of a cryogenic target,[12,13] images were obtained from three sets of the phosphor coupled with the CCD cameras. Four pinhole images through aluminum filters with different thicknesses of 2, 3, 6, 10 μm were arranged on each phosphor. The diameter of each pinhole was normally 20 μm and the magnification of pinhole camera was 8. The target was a foam shell with an outside diameter of 780 μm and a wall thickness of 35 μm filled with liquid deuterium. Twelve laser beams from a frequency-doubled Gekko XII glass laser system were focused onto the target with a pulse duration of 1 ns and a total energy of 8 kJ.

Figure 4 shows the isotemperature surface at 450 keV in the core. In the present status of the cryogenic experiments, it is very difficult to fill the foam shells with deuterium completely and uniformly; the resultant cores are severely distorted in some cases. Although the 2-D x-ray image was somewhat round and more uniform, the reconstructed temperature was shown to have a nonuniform distribution as in Fig. 5. In this shot, the core temperature ranged from 200 to 1000 eV. Since the inferred temperature is proportional to the intensity ratio R to the power of 1.7, the error in the calculated temperature is estimated to be 30% due to the reconstruction error in the intensity distribution.

The experimentally measured areal density ρR of the compressed core of the cryogenic foam shell was < 10 mg/cm^2 and the temperature was much higher than the ionization energy of carbon (which has the highest Z number in the target). Therefore all the assumptions we described previously were fulfilled.

The reconstruction of the temporally resolved 3-D x-ray image was demonstrated using two sets of the identical x-ray framing cameras. Each framing camera was arranged to provide six sequential images with a time interval of 100 ps. The timing jitter of two sets of the x-ray framing cameras was measured by monitoring driving electric pulses on a 6 GHz digitizing oscilloscope (Tektronix 7250). Practically two sets of detectors are not sufficient to perform the tomographic reconstruction. $\langle \delta I/I \rangle$ was calculated to be larger than 50% using a phantom simulating a spherical shell plasma. We defer detailed analysis until we have finished the installation of three sets of the x-ray framing cameras and we fully understand reconstruction artifacts on the distinctive shapes. In order to discuss the evolution of the deformation of the shell and corresponding nonuniformity of the compressed core, it is necessary to expand the distribution to a proper set of orthogonal functions.

IV. SUMMARY

The x-ray emission CT system has been constructed using phosphor (Zn, Cd)S:Ag as a time-integrated detector and an x-ray framing camera as a temporally resolved detector in order to investigate the three-dimensional nonuniformity of the imploding pellet target in an inertial confinement fusion experiment. Reconstruction accuracy was evaluated by computer simulation using a phantom of a compressed core. Deviation in intensity and spatial resolution were estimated to be 20% and 40 μm, respectively, in the case of using three detectors. 3-D distributions of electron temperature and density were reconstructed using an absorption filter technique. We successfully applied this system to measure implosions of cryogenic targets. In order to study the 3-D evolution of the target nonuniformity, it is essential to expand the distribution of the physical parameter to a proper set of orthogonal functions. From this point of view the reconstruction accuracy must be evaluated.

[1] N. M. Ceglio and L. W. Coleman, Phys. Rev. Lett. **39**, 20 (1977).
[2] Y.-W. Chen, N. Miyanaga, M. Yamanaka, H. Azechi, K. Nishihara, Y. Kato, T. Yamanaka, and S. Nakai, J. Appl. Phys. (to be published).
[3] G. T. Herman, A. Lent, and S. W. Rowland, J. Theor. Biol. **42**, 1 (1973).
[4] R. Rangayyan, A. P. Dhawan, and R. Gordon, Appl. Opt. **24**, 4000 (1985).
[5] M. R. Civanlar and H. J. Trussell, ICASSP **86**, Tokyo (1986).
[6] Y.-W. Chen, N. Miyanaga, M. Yamanaka, M. Nakai, K. A. Tanaka, K. Nishihara, T. Yamanaka, and S. Nakai, J. Appl. Phys. (to be published).
[7] A. J. Duerinckx and A. Macovski, IEEE Trans. Nucl. Sci. **NS-26**, 2848 (1979).
[8] A. Macovski, Proc. IEEE **71**, 373 (1983).
[9] J. H. Kinney, Q. C. Johnson, U. Bonse, R. Nusshardt, and M. C. Nichols, SPIE **691**, 43 (1986).
[10] S. Gruner, Rev. Sci. Instrum. **60**, 1545 (1989).
[11] M. Katayama, M. Nakai *et al.*, Proc. of European Conf. on Optics, 24–28 April, Paris, 1989. This camera has been developed in ILE and manufactured at Hamamatsu Photo., K. K.
[12] T. Norimatsu *et al.*, J. Vac. Sci. Technol. A **6**, 3144 (1987).
[13] T. Yamanaka *et al.*, in *Laser Interaction with Matter*, edited by G. Velarde, E. Minguez, and J. M. Perlado (World Scientific, Teaneck, NJ, 1989).
[14] Y. Kato *et al.*, ILE Quarterly Progress Report, ILE-QPR-84-8.